DYNAMICALY BALANCED DEGENERATE MODE GYRO WITH SUB-HZ FREQUENCY SYMMETRY AND TEMPERATURE ROBUSTNESS

J. Giner[1], Y. Zhang[1], D. Maeda[1], K. Ono[1], A.M. Shkel[2] and T. Sekiguchi[1]
[1]Hitachi. Ltd, R&D Group, Kokubunji, JAPAN
[2]Microsystems Laboratory, University of California, Irvine, USA

ABSTRACT

We designed, fabricated, and experimentally demonstrated a dynamically balanced z-axis MEMS vibratory gyroscope utilizing the concentrated suspension architecture. This architecture allows for a high degree of structural symmetry (degeneracy of modes), potentially enabling high precision Rate Gyroscopes (RG) and Rate Integrating Gyroscopes (RIG). The full dynamic balance of the design is enabled by two concentric masses that oscillate in anti-phase as an unconstrained tuning fork, in any direction in-plane of the substrate. Experiments demonstrated a sub-Hz, as fabricated, frequency split (Δf) of 190mHz (0.19Hz) confirming the objective of the architecture. The high level of symmetry makes the gyro robust against temperature variations, demonstrating less than 50mHz variation of Δf in a broad range of temperatures, from -30^{0}C to 100^{0}C.

INTRODUCTION

Dynamically balanced, degenerate-mode silicon MEMS gyroscopes, [1, 2], are the candidates for precision rate and rate integrating operation. This technology will be required for GPS-denied navigation, precision pointing, and platform stabilization. The increase in performance of MEMS Coriolis vibratory gyroscopes depends largely on the ability to achieve and maintain the frequency separation between the drive and sense modes, approaching Δf=0. Non-zero Δf degrades the performance of the device (Figure 1) by increasing the Mechanical Thermal Noise limit in RG and the angle drift in RIG modes of operation, [3].

Degenerate mode gyroscopes are designed to have the same drive and sense frequencies. However, several steps of the fabrication process, such us lithography and etching, introduce asymmetries in mass and stiffness. Suspension springs are especially critical element of the design since any change in width or slope of the etching strongly affects the resonance frequency of the two operational modes, thus increasing the frequency separation.

In practice, with the current state-of-the-art silicon etching technology, it is not possible to obtain a perfect as-fabricated mode-matched gyroscope. Post-fabrication frequency tuning mechanisms are put in place to reduce the frequency asymmetry. These frequency tunning techniques can be classified in two groups, as mechanical and electric/electronic. Mechanical perturbations can be based on mass removal from suspension springs using UV laser, allowing to modify the stiffness of a particular mode and hence its resonant frequency [4]. Alternatively, the compensating perturbations can be based on a mass addition,

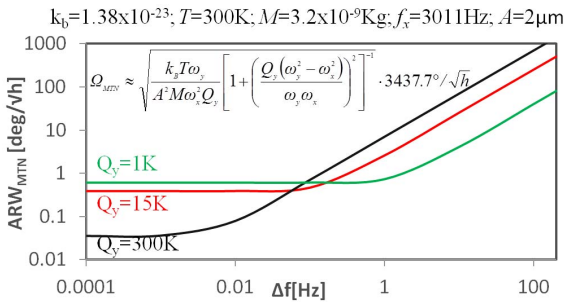

Figure 1: Angle Random Walk (ARW) of RG as a function of Q-factor and Δf.

for example, in the form of silver-nano-particles ink droplets in reservoirs strategically placed to reduce the resonant frequency of a certain mode. With the mass addition approach, the as-fabricated frequency split of 14Hz can be reduced to less than 1 Hz, [5]. These techniques require an individual treatment of each resonator since it has to be done before packaging, making the post processing long and costly, and potentially damaging the device if the process is not well controlled.

A more flexible alternative is based on electrostatic tuning of the operational modes. In [6], an automatic frequency matching circuit based on the phase relationship between the residual quadrature and drive signals provides a DC voltage that is applied to electrodes to reduce the frequency split. Stability of the voltage source is critical to define the limits of symmetry that can be achieved. In cases with large Δf, a large tuning voltage is required. The voltage increase has a negative effect on other structural parameters, such as the Q-factor. It was also reported that a voltage required to tune a large as-fabricated mismatch might result in dynamic misbalance dynamic balance of the mechanical device [7]. In cases with a smaller as-fabricated frequency split, the displacement feedback can be applied to achieve the frequency splits around 10mHz, [8].

In this work, we approach the problem of the frequency mismatch by addressing the issue at the design stage. Specifically, we explored the idea of concentrating the critical parts of the design – the suspension elements – in a small central area of the device. This design strategy allowed us to mitigate a non-uniformity of etching and led to highly isotropic gyro structures. Our literature survey (Figure 2) suggested that as-fabricated non-zero *Δf* can be reduced if the suspension springs are located in a small area (A_s), as compared to the device area (A_d). The design was first introduced in [9], where the Q-factor above 300K was demonstrated. In this work, we also report an intriguing

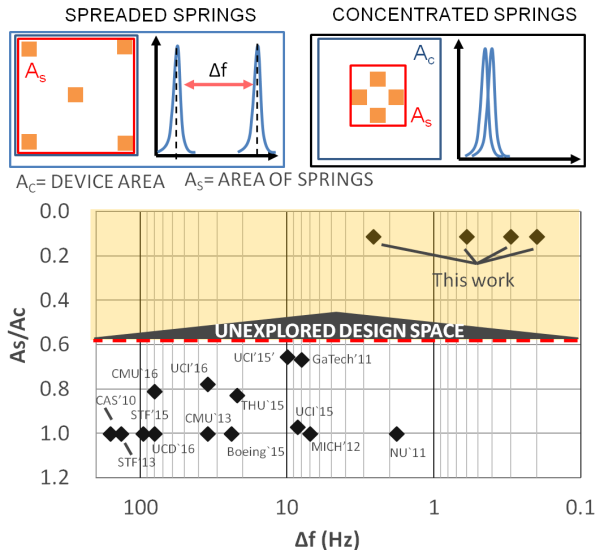

Figure 2: Literature survey mapping approaches based on concentration of structural anchors. Simplified schematics of MEMS gyroscopes highlights the area of the footprint (A_c) and the area of suspension springs (A_s)

property of the symmetric design architecture to preserve the as-fabricated frequency separation, *Δf*, despite a wide range of variations in temperature.

ARCHITECTURE

The design reported in this paper is based on two mechanically coupled concentric circular masses that share the same center of mass. Both proof-masses are designed to have the same mass and the same resonant frequencies. Masses are attached to the substrate by 4 anchors. The anchors are located in between the two masses and mechanically connected to the masses via a pair of shuttles. The shuttles are connected to the inner and outer masses by suspension springs and are constrained to move in one degree of freedom, while allowing at the same time the inner and the outer mass to move freely in any direction on the XY plane. Figure 3 shows a schematic representation of the dynamics of the resonator in operation.

When in operation, the masses are forced to oscillate in an out-of-phase in x- or y- modes (a tuning fork-like motion), by using electrostatic electrodes embedded inside the suspended masses. For the inner and outer masses, the same frequency of operation is achieved by implementing the coupling springs between the inner and the outer shuttles. During the operation, the two pairs of shuttles moves in an out-of-phase motion with respect to the anchor and along the respective mass, while the equivalent and perpendicularly oriented pairs remain motion-less. Like in a conventional tuning fork, the center of masses of the presented design remains cantered during the operation, canceling reaction torques and forces in anchors, thus mitigating the mechanical energy leakage through the anchors.

Electrostatic actuation and capacitive sensing are

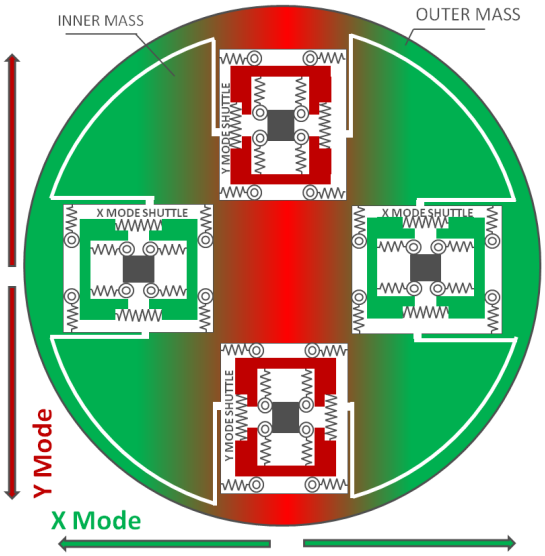

a)

Figure 3: Diagram of dynamically balanced z-axis gyroscope with concentrated suspension springs. Monochromatic parts move in one direction (1 DoF) and dichromatic parts are free to move in any direction in the XY plane.

possible due to 32 electrodes embedded in the masses, 16 for the inner mass and 16 for the outer mass. To allow a large displacement of the masses, the gap of the parallel plates is 8µm. The total capacitance is 10pF.

In our design approach, the key element of the design is a compact architecture of the spring-shuttle-anchor module. In the presented design implementation the area of the suspension spring, $A_{s,}$ is 2x2µm, and the area of the sensing element, A_c, is 5.7x5.7µm, providing a ratio of A_s /A_s=0.2. Per our survey of literature, Figure 2, this is the lowest ratio report in the literature, and is believed to be a critical design parameter.

EXPERIMETAL RESULTS

Fabrication

An array of devices is fabricated using a single mass standard 6" SOI process with a 60 µm device layer thickness and 2 µm buried oxide. A stepper was used to define three different patterns of suspension springs with widths of 3, 5 and 10µm resulting in 1.2, 3, and 10kHz resonance frequencies, respectively. Structures were released using the vapor HF through the release holes, defined on the mass and on the shuttles. Figure 4 shows the top view of the released devices.

Resonator characterization

Released devices were attached to ceramic packages using conductive epoxy. A pair of electrodes of the inner mass and a pair of electrodes of the outer mass were used for excitation per each axis and the same number of electrodes

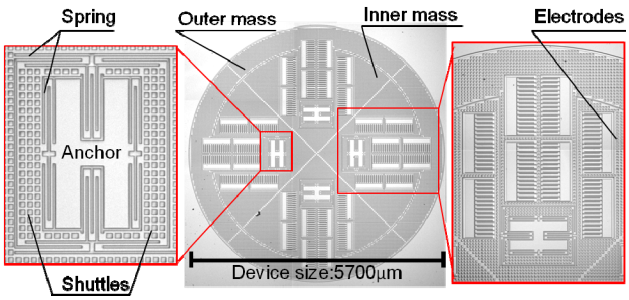

Figure 4: Optical image of the gyroscope and close up of electrodes and spring-shuttle anchor module

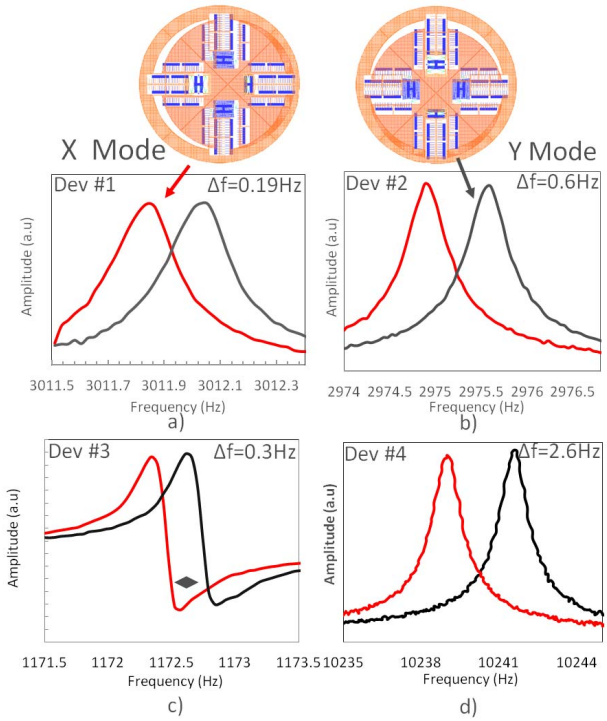

Figures 5. Measured Δf for devices with different spring width of 5μm in a) and b), 3μm in c), and 10μm in d).

were used for pick off (1.2pF actuation and 1.2pF sense capacitances). The device was tested in a custom-built vacuum chamber and external amplifiers by Zurich Instruments (HF2TA) were used to transform the motional current with the gain of 100KΩ. Zurich Instrument HF2FL was used to characterize drive and sense modes. A carrier frequency along with a 6V continuous voltage was applied to the suspended masses. The AC voltage of 100mV was applied to the forcer electrodes, first in the X mode followed by excitation of the Y mode. Results are shown in Figure 5.

Temperature stability

The device was vacuum packaged at moderate vacuum, with the pressure around 5 Pa, and then placed inside the thermal chamber ESPEC SH-240 with a temperature control from -30°C to 100°C. The thermal chamber was manually controlled. After setting the reference temperature we

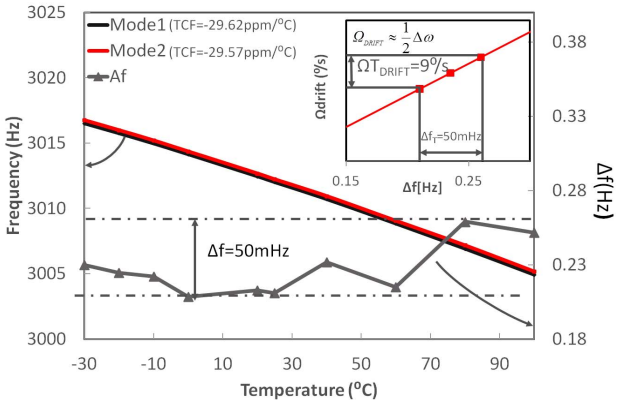

Figure 6: TCF and Δf characterization. Concentrated anchor provides 0.12ppm/C° stability of the frequency split. Inset shows the effect of the TCF on the angle estimation (we assumed Δ(1/τ)=0).

allowed 30 min for the MEMS to thermally stabilize. The resonant frequencies of the drive and sense mode were recorded during the incremental temperature sweep. The high symmetry was achieved thanks to the concentrated suspension design. The measured temperature coefficient of resonant frequency (TCF) was measured 29.62ppm/°C for the sense mode and 29.57ppm/°C for the drive mode, and the frequency symmetry variation was only 50mHz. For Rate Integrating Gyroscope mode of operation the angle drift is limited by anisodamping and can be estimated using

$$\Omega_{drift} \approx \frac{1}{2}\Delta\frac{1}{\tau}+\frac{1}{2}\Delta\omega \qquad (1)$$

For simplicity, we assume 1/τ=0, the angle drift due to the thermal effects was estimated 9°/s.

Open-loop gyroscope characterization

The device was instrumented as a gyroscope. The FPGA-based lock-in amplifier HF2LI was used to implement all the control loops. The drive oscillation control was implemented with PLL and AGC to ensure an out-of phase vibration of the microsystem is around 2μm. The device was placed on a custom-built rate table with sinusoidal- and square- rate input capabilities. The Y-axis pick-off electrodes were connected to the lock-in amplifier via trans-impedance amplifiers HF2TA. To mitigate the parasitic capacitance, the Electromechanical Amplitude Modulation (EAM) scheme was used. The Δf was electrostaticaly tuned by applying -2.2VDC to the Y-mode forcer electrodes to reach Δf=50mHz. The tuning voltage can be reduced by a half if both the forcer and pick off electrodes are used. The Q-factors for the drive and sense modes were around 10,000.

The rate table was rotated at +/-5, +/-10, and +/-20 °/s and the gyro output was recorded (Figure 7). The experimentally derived Scale Factor (SF) is 24.6μV/°/s. The Zero Rate output was recorded for 3000 seconds with the 3.51Hz sampling rate. The Allan Variance in physical units showed the noise level in the form of the Angle Random Walk (ARW) of 5.4°/√Hz and the Bias Stability of 25°/h at

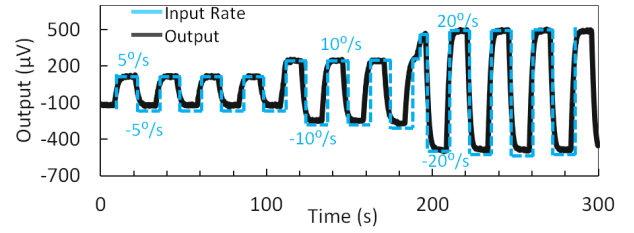

a)

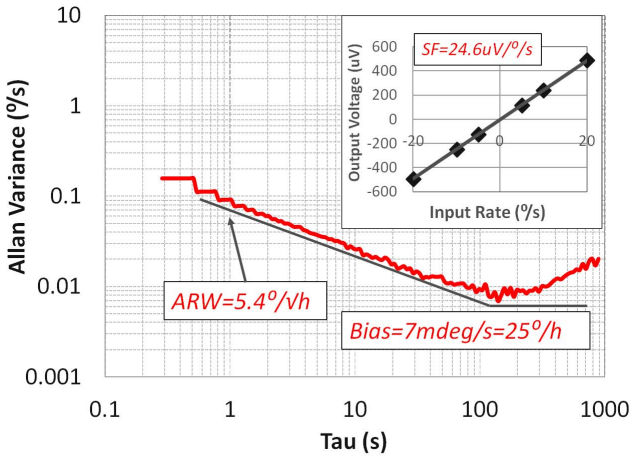

b)

Figure 7: a) Output of open-loop gyroscope under rotation with frequency of 200mHz. b) Allan variance in physical units is from 3000sec of data. Inset shows the scale factor in open loop with no quadrature null.

room temperature, without the temperature control and quadrature null.

CONCLUSIONS

A new architecture of a z-axis MEMS gyroscope is presented. The key feature of the architecture is the use of concentrated suspension springs in a small area around the center of the device, with an objective to mitigate the imperfections introduced by the fabrication process and preserve the frequency symmetry of device through operation. A sub-Hz as-fabricated frequency symmetry has been consistently observed on devices. The best as-fabricated frequency symmetry of Δf=0.19Hz was obtained for a device with 3,011 Hz nominal frequency. The device was vacuum packaged at 5 Pa and experimentally demonstrated to maintain the 50mHz frequency symmetry. The open-loop gyroscope characterization showed the in-run bias drift of 25°/h. We expect to improve the noise performance by operating the gyroscope at the Q- factors of 300K; which has been demonstrated by the group for the introduced architecture [9].

ACKNOWLEDMENTS

Authors would like to thank the invaluable help of Takashi Shiota from Hitachi for fabricating devices and to Hideyuki Maekoba from CoventorWare for help with MEMS+.

REFERENCES

[1] D. Senkal, A.Efimovskaya, A.M. Shkel, "Minimal realization of dynamically balanced lumped mass WA gyroscope: dual foucault pendulum," *The 2015 IEEE International Symposium on Inertial Sensors and Systems (IEEE INERTIAL 2015),* Hapuna Beach, HI, USA, March 23-26, 2015

[2] A. A. Trusov, G. Atikyan, D.M. Rozelle, A.D. Meyer, S. Zotov, B.R. Simon, A.M. Shkel, "Force rebalance, whole angle, and self-calibration mechanization of silicon MEMS quad mass gyro," *The 2014 IEEE International Symposium on Inertial Sensors and Systems (IEEE INERTIAL 2014)*, Laguna Beach, CA, USA, Feb 25-26, 2014

[3] D. D. Lynch, "MRIG frequency mismatch and quadrature control," *2014 International Symposium on Inertial Sensors and Systems (IEEE INERTIAL 2014),* Laguna Beach, CA, 2014,

[4] Z. Hou, X. Wu, D. Xiao, X. Wang and Z. Chen, "Modal coupling error suppression in micromachined gyroscopes by UV laser trimming," *IEEE SENSORS,* Busan, 2015

[5] D. Kim, R. M'Closkey, "A MEM vibratory gyro with mode-matching achieved by resonator mass loading," *2014 IEEE/ION Position, Location and Navigation Symposium - PLANS 2014*, Monterey, CA, 2014

[6] S. Sonmezoglu, S. E. Alper and T. Akin, "A high performance automatic mode-matched MEMS gyroscope with an improved thermal stability of the scale factor," *2013 Transducers & Eurosensors XXVII: The 17th International Conference on Solid-State Sensors, Actuators and Microsystems (TRANSDUCERS & EUROSENSORS XXVII)*, Barcelona, 2013

[7] S. Askari, M. H. Asadian, K. Kakavand and A. M. Shkel, "Vacuum sealed and getter activated MEMS Quad Mass Gyroscope demonstrating better than 1.2 million quality factor," *The 2016 IEEE International Symposium on Inertial Sensors and Systems (IEEE INERTIAL 2016),* Laguna Beach, HI, USA, Feb 22-25, 2016

[8] Z. X. Hu, B. J. Gallacher, J. S. Burdess, C. P. Fell and K. Townsend, "Precision mode matching of MEMS gyroscope by feedback control," *IEEE Sensors*, Limerick, 2011

[9] J. Giner, Y. Zhang, D. Maeda, K. Ono, S. Kajiyama, T. Oshima, T. Sekiguchi, T. Yamawaki "Concentrated springs architecture for single digit frequency Split in Silicon Gyroscopes" *IEEE SENSORS,* Orlando, 2016

CONTACT

*J.Giner tel:+81-70-2676-7544;
joan.giner.od@hitachi.com